



*Institute of Paper Science and Technology
Atlanta, Georgia*

IPST Technical Paper Series Number 832

NPE Modeling of a Laboratory Bleach Filtrate Recycle Experiment

A. Rudie, A. Puckett, and G.L. Rorrer

December 1999

Submitted to
AIChE Meeting
1999 TAPPI Pulping Conference
October 31–November 3
Orlando, Florida

Copyright© 1999 by the Institute of Paper Science and Technology

For Members Only

INSTITUTE OF PAPER SCIENCE AND TECHNOLOGY PURPOSE AND MISSIONS

The Institute of Paper Science and Technology is an independent graduate school, research organization, and information center for science and technology mainly concerned with manufacture and uses of pulp, paper, paperboard, and other forest products and byproducts. Established in 1929, the Institute provides research and information services to the wood, fiber, and allied industries in a unique partnership between education and business. The Institute is supported by 52 North American companies. The purpose of the Institute is fulfilled through four missions, which are:

- to provide a multidisciplinary education to students who advance the science and technology of the industry and who rise into leadership positions within the industry;
- to conduct and foster research that creates knowledge to satisfy the technological needs of the industry;
- to serve as a key global resource for the acquisition, assessment, and dissemination of industry information, providing critically important information to decision-makers at all levels of the industry; and
- to aggressively seek out technological opportunities and facilitate the transfer and implementation of those technologies in collaboration with industry partners.

ACCREDITATION

The Institute of Paper Science and Technology is accredited by the Commission on Colleges of the Southern Association of Colleges and Schools to award the Master of Science and Doctor of Philosophy degrees.

NOTICE AND DISCLAIMER

The Institute of Paper Science and Technology (IPST) has provided a high standard of professional service and has put forth its best efforts within the time and funds available for this project. The information and conclusions are advisory and are intended only for internal use by any company who may receive this report. Each company must decide for itself the best approach to solving any problems it may have and how, or whether, this reported information should be considered in its approach.

IPST does not recommend particular products, procedures, materials, or service. These are included only in the interest of completeness within a laboratory context and budgetary constraint. Actual products, procedures, materials, and services used may differ and are peculiar to the operations of each company.

In no event shall IPST or its employees and agents have any obligation or liability for damages including, but not limited to, consequential damages arising out of or in connection with any company's use of or inability to use the reported information. IPST provides no warranty or guaranty of results.

The Institute of Paper Science and Technology assures equal opportunity to all qualified persons without regard to race, color, religion, sex, national origin, age, disability, marital status, or Vietnam era veterans status in the admission to, participation in, treatment of, or employment in the programs and activities which the Institute operates.

NPE Modeling of a Laboratory Bleach Filtrate Recycle Experiment

Alan Rudie¹, Ana Puckett¹, and Gregory L. Rorrer²

¹ Institute of Paper Science and Technology

² Department of Chemical Engineering, Oregon State University

ABSTRACT

Nonprocess elements such as calcium, barium, and manganese build up in fiber lines because they are released from binding sites on fibers into the filtrate at acid pH and adsorb back onto the fibers at neutral and alkaline pH. They can also precipitate as hydroxides and carbonates under alkaline conditions and as sulfates and oxalates under acidic conditions. This project used a laboratory filtrate recycle experiment with 10 full D₀(EP)D bleaching cycles and a direct countercurrent wash scheme to evaluate the buildup of NPE's and provide a database for testing selectivity coefficient adsorption equilibrium constants in a process model. Calcium and sodium concentrations were found to continue to increase in the D₀ filtrates through all ten bleach cycles and showed no evidence of approaching a process equilibrium. Barium shows a surprising decline in concentration in the D₀ filtrate after 7 cycles. Magnesium and manganese show little buildup after the first cycle.

Two model approaches have been evaluated. OLI systems ESP software was used to calculate the stream compositions of the 10th bleach cycle. This model is capable of estimating the majority of the potential NPE speciation in the bleach plant streams as well as metal adsorption and precipitation. The model predicts precipitation of calcium carbonate in the extraction stage and calcium oxalate and barium sulfate in the D₀ stage of bleaching. The second model used an Excel spreadsheet and Visual Basic macro's to calculate the adsorbed and dissolved metal concentrations. This method does not consider competition with other anions but was capable of modeling the buildup of NPE's through all ten cycles of the lab study.

Submitted to AIChE for 2000 Symposium series.

Contacts are:

- Greg Rorrer, Dept. of Chemical Engineering, 103 Gleeson Hall, Oregon State University, Corvallis, Oregon 97331-2702: rorrergl@che.orst.edu
- Alan Rudie, Institute of Paper Science and Technology, 500 Tenth St. N.W., Atlanta, Georgia 30318-5794: alan.rudie@ipst.edu

INTRODUCTION:

Trace metals build up in bleach plants through a mechanism involving the ion exchange properties of wood pulps,^{1,2} the alternating pH in the bleach plant, and the recycle of bleach filtrates. Since barium, radium, and manganese are not needed in the process, and calcium is unwanted in the pulping and bleaching process, these metals and others that routinely accumulate with them are collectively referred to as nonprocess elements (NPE). NPE's are responsible for mineral scales (barium/radium sulfate, calcium oxalate, and calcium carbonate)^{3,4} and decomposition of some bleaching chemicals (manganese).² Recent changes in mills have exacerbated the NPE problems,⁵ and continuing efforts to reduce wastewater discharge can only make the problem worse. For these reasons, it is imperative to get a better understanding of trace metal behavior and develop the capability to model and predict metal accumulation.

Metal ions in solution reversibly bind to functional groups on wood pulp by an ion exchange mechanism. In kraft pulps, the carboxylic acid groups on the pulp serve as the primary adsorption sites for metal cations⁶ although phenolic hydroxyl groups can also bind with metal⁷ ions at pH greater than 10. In the ion exchange process, acid groups on the fibers lose a proton to the external solution. This results in a buildup of negative charge, which attracts cations and repels anions. This attraction for cations prevents any significant buildup of charge on the fiber and results in – for practical purposes – a one-to-one match of ion exchange sites and cation charge in the fiber. A small negative charge remains, but it can only be measured by charge mobility techniques like zeta potential, and it cannot be measured analytically.⁸

Typical carboxylic acids have a pKa around four, and this pH is about the midpoint of the pH sensitivity of wood fibers.⁷ At pH's below 4, metals are displaced from the fibers by protons. At pH above 4, there are too few protons in solution to compete for the carboxylic acid sites, and metal cations are adsorbed from solution. The chlorination stage typically operates at a final pH near 1.5. At this pH, 99% or more of the carboxylic acids are protonated and trace metals are effectively stripped from the fibers and released with the discharge from the chlorination stage filtrate tank. A ClO₂ stage operates at a discharge pH closer to 3. This higher pH has a number of contributing factors to increase scale formation. The second pKa for oxalic acid ($\text{HC}_2\text{O}_4^- \rightarrow \text{C}_2\text{O}_4^{2-} + \text{H}^+$) and sulfuric acid ($\text{HSO}_4^- \rightarrow \text{SO}_4^{2-} + \text{H}^+$) are 4.3 and 2, respectively.⁹ The increase in pH from 1.5 to 3 results in a 300% increase in the concentration of sulfate anions (versus HSO_4^-) and a 1000% increase in the concentration of oxalate anions (versus HC_2O_4^-). At pH 3, about 10% of the acid groups are still occupied by trace metals. Since the ion exchange preference for cations favors high charge, divalent cations like calcium and barium are significantly favored over monovalent cations like sodium.¹ This results in a ten-fold increase in carryover of calcium and barium into the rest of the bleach plant, increasing the risk of calcium carbonate scaling in the extraction stage.

This effort comprises a number of tasks necessary to improve the ability to understand, predict, and eventually control the buildup of trace metals in the fiberline. First, the partition of trace metals between fiber and solution must be measured under controlled conditions and must be described or accurately modeled as a chemical equilibrium. The approach taken in this effort was to measure and characterize the competition between cations for binding sites on the fibers. These were successfully described in terms of selectivity coefficients, an equilibrium formalism that is fairly similar to solution equilibrium theory. Second, a data set was needed to provide a test of the selectivity coefficients and modeling methods. To accomplish this, a ten-cycle laboratory bleaching filtrate recycle experiment was undertaken. A laboratory provides a more stable environment for collecting data and also provides the capability of monitoring the buildup of trace metals in the process in a stepwise fashion. The alternative, comprehensive mill sampling, rarely obtains a true picture of a stable “equilibrium” system because of the continual process drift. Finally, two modeling approaches have been evaluated. A spreadsheet model was developed to calculate the stepwise buildup in trace metals through the ten cycles. This model can calculate the distribution of trace metals between the pulp and filtrate, but does not consider formation of soluble complexes or precipitation. The second model uses the OLI Systems Inc. equilibrium software ESP. This software uses mix, separation, and sorption blocks in an equilibrium and material balance calculator. It was used to evaluate the distribution of metals in the tenth cycle using the filtrates from the ninth cycle.

EXPERIMENTAL:

Selectivity coefficients for metal adsorption were determined using a modification of the procedure reported by Diniz.¹⁰ The fines were removed from a commercial sample of southern pine linerboard grade pulp by diluting to below 1% consistency and thickening over a 100 mesh sidehill screen. This process was repeated until the remaining fines content (pass 100 mesh) was below 2% as measured by the Bauer McNett Classifier. The pulp was then diluted to 3% consistency with deionized (nano-pure) water. Sufficient hydrochloric acid was added to reduce the pH to 1.5, and the pulp suspension was heated to 65° C for 90 minutes. The pulp was washed thoroughly with deionized water and diluted back to 3% consistency. Sufficient metal chloride was added to raise the cation concentration to 0.01 molar, and the pH was raised above 8.0 with either sodium hydroxide or tetramethyl ammonium hydroxide. After 90 minutes, the pulp was filtered and washed with deionized water. The pulp was then diluted to 3% consistency with deionized water and allowed to soak overnight. The pulp was filtered to 20% consistency and stored in a cold room at 4° C until needed. With care to avoid contamination, this procedure resulted in a pulp with 90% or more of the ion-exchange sites occupied by the primary metal selected for the study.

The competition experiments were carried out by diluting 3 g O.D. of pulp to 1% consistency and adding a known concentration of the competing metal (the only source of primary metal was the metal bound to the starting pulp). The pH was checked to make sure it was near neutral, and the slurry was stirred for 30 minutes using an overhead stirrer with a U-shaped polyethylene paddle. The pulp was then collected on a Büchner funnel and pressed between blotters in a Tappi sheet press at 98 psig for 5 minutes. This elevated the pulp consistency to about 40% and greatly decreased the amount of “external” solution that needed to be accounted for in the calculations. Pulp samples were weighed, dried, and analyzed by ICP.¹¹ Typically, the competing metal concentration was varied between 10⁻⁴ to 0.1 mole/L for these experiments.

Acid group content and total metal input of the primary cation is known from the starting pulp analysis and amount of pulp used in the exchange reaction.¹² Total secondary metal added is also known. Adsorbed metal is determined from the exchanged pulp analysis, and the solution concentrations can be determined by difference.

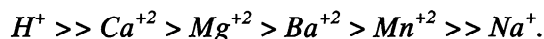
One problem with ion exchange equilibria is that the adsorbed ions are technically at a different concentration from the external solution and this concentration is subject to the swelling and shrinking of the ion exchange media. In cases where the competing ions do not carry the same charge, the concentration terms do not cancel and the concentration assumption becomes part of the equilibrium constant. There are several formalisms for representing the concentration basis of the bound metal.¹³ For OLI, the bound concentration is determined on a total solution basis. For the Excel spreadsheet model, selectivity coefficients are evaluated on a charge fraction basis, where charge fraction is the fraction of ion-exchange sites neutralized by a particular ion. Using charge fraction, the units on the selectivity coefficient become Mole/L for the case with a divalent and a monovalent cation. (The concentration assumption still cancels when the results are analyzed on a total solvent basis.) The term selectivity coefficient will herein be used to refer to the constant obtained using the charge fraction formalism. Equilibrium constants will be used to refer to the constant obtained when bound concentrations are calculated on a total aqueous phase basis since this formalism is equivalent to the aqueous solution convention.

Equilibrium constants for H-Ca, Na-Ca, Mg-Ca, Ba-Mg, and Mn-Mg exchange on brownstock pulp were estimated from the log-log distribution plots presented in *Figures 1* and *2*. For convenience, the common adsorbed ion (Ca-pulp or Mg-pulp) is provided on the x-axis. However, for regression analysis, the displacement ion was always the independent variable. For example, concentration data from Na-Ca exchange experiments were analyzed by linearization of the mass action expression

$$\log \left(\frac{[Ca \cdot R_2]}{[Ca^{+2}]} \right) = n \cdot \log \left(\frac{[Na \cdot R]}{[Na^+]} \right) + \log K^{Ca/Na} \quad (2)$$

where R represents the carboxylate ion-exchange site on the pulp and the quantities in the brackets represent molar concentrations of the metals on the pulp and in solution. Estimates for binary equilibrium constant K and molar equivalent ratio n from the least-squares slope and intercept of the regression

analysis are presented in *Table 1*. In *Figures 1* and *2*, the intercept is graphically represented with respect to the x-axis. Binary equilibrium constants were scaled to a common Ca^{+2} exchanged basis using the Triangle Rule as summarized in *Table 2*.¹⁴ From the K values given in *Table 2*, the order of affinity for binding of cations on pulp is:



This is very similar to the binding preference reported by Ohlsson and Rydin.¹ Based on the sequence above, H^+ is the most strongly bound cation whereas Na^+ is the most easily displaced cation. The divalent metal ions have equilibrium constants on the same order of magnitude, and they will actively compete with one another for ion-exchange sites on the pulp. Equilibrium constants for ion exchange are only a weak function of temperature¹⁵ so the K values in *Table 2* were presumed valid in the 25 to 70°C temperature range. This has been verified with experiments on select metal ion pairs. Values for n generally agreed with the theoretical stoichiometry, except for H-Ca exchange on pulp. Laine contends the lack of fit to the theoretical stoichiometry of 2 for proton exchange is due to the presence of two different carboxylic acid sites with pK_a 's of 3.36 and 5.42.¹⁶

The Selectivity Coefficients used in the Excel model were obtained in a similar fashion, except:

1. The stoichiometric term was adjusted to an integer value: 1 for hydrogen exchange, 2 for sodium exchange, and 1 for all the divalent metals.
2. The final selectivity coefficient was optimized to match the equilibrium point of the competition experiments rather than the best fit of the log data.
3. Selectivity coefficients included Debye Hückel estimates of the activity in the fitting procedure since this becomes significant at ionic strengths above 0.001M.¹⁷

The selectivity coefficients used in the Excel model are also listed in *Table 2*. The differences in K values for exchange with H^+ and Na^+ are due to the differences in concentration assumptions and the use of integer values for the stoichiometry coefficient n . The differences in the divalent cations are not overly significant, but they do indicate a change in the order of binding preference with Mn^{2+} , binding more strongly than Mg^{2+} and Ba^{2+} .

The bleach filtrate recycle experiment attempted to mimic an OD(EP)D bleach line with direct countercurrent use of wash water. Closure to the pulp mill was included by using D_0 stage filtrate as wash water on a simulated oxygen stage washer. This was accomplished by diluting 75 ODg of oxygen bleached pulp to 3% consistency and adjusting the pH to >10.5. The pulp was thickened on a Büchner funnel to a nominal 12% consistency and then washed with 660 ml of D_0 filtrate collected from the previous D(EP)D bleach cycle. Final pulp weight was checked, and if the consistency was above 12%, it was diluted back to 12% with oxygen stage filtrate.

Two different pulp samples were used in the bleach filtrate recycle experiments. Sample 1 was a commercial sample of oxygen-bleached mixed southern hardwood pulp with a Kappa number of 12.5 and 15.9 mPa·sec viscosity. This was used for the first two cycles of the experiment. Sample 2 was an oxygen-bleached hardwood from the same mill but with a starting Kappa of 9.8 and initial viscosity of 18.9 mPa·sec. The starting metals content of the two pulps is reported in *Table 3*.

Bleaching experiments were carried out in Kapak heat-sealed bags using the conditions summarized in *Table 4*. All wash stages were carried out as indicated above. A 120 ml filtrate sample was collected from each acid filtrate and a 12 ml sample from the EP filtrate. A 10 g O.D. sample of pulp was collected after the EP stage. Chemical addition provided sufficient make-up to maintain the filtrate balance without the need for fresh water.

RESULTS

Extracted pulp kappa number and bleached pulp brightness and viscosity are reported in *Table 5*. The extracted kappa is within the normal range, and bleached brightness reached the target level of 84-85 in the third cycle. The increase in brightness after the second cycle was probably due to the change in starting pulps. For the first two cycles, the first stage chlorination factor was 0.21; for the final 8 stages, it was rather high at 0.27.

In a direct countercurrent filtrate recycle bleach plant, the D_0 filtrate and D_1 pulp are the two outlets for trace metals. In this experiment, D_0 filtrate was used as wash water on the simulated oxygen stage washer, so the oxygen stage filtrate is the soluble NPE outlet from the process. In a fully closed

sequence, even this outlet is eliminated because the filtrate continues to be recycled to brownstock washing and the NPE's either end up adsorbed or precipitated on fiber, or remain in the aqueous phase and end up in recovery. The D₀ stage still represents the high concentration point for NPE's and the most likely place for acid stable scales like barium sulfate and calcium oxalate.

The buildup of trace metals in the D₀ filtrate of the bleach filtrate recycle experiments is shown in *Figures 3* for calcium and sodium and *Figure 4* for magnesium, barium, and manganese. Calcium builds up from a starting concentration of 50 ppm in cycle 1 to 250 ppm by the tenth cycle. Similarly, sodium rises from 20 to 200 ppm over the ten cycles. Neither calcium or sodium shows any significant change in slope that would indicate the metals are approaching a process equilibrium concentration. In contrast, magnesium, barium, and manganese appear to have reached an equilibrium status at about the fifth cycle (*Figure 4*). This may be evidence of precipitation of BaSO₄ in D₀ and Mg(OH)₂ and Mn(OH)₂ in the extraction stages and retention of much of the precipitate on the fibers. The barium concentration actually declines after the 7th cycle.

The buildup of trace metals on D₁ pulp is shown in *Figure 5* for calcium and sodium, and *Figure 6* for magnesium, barium, and manganese. The D₁ stage pulp analysis is the sum of bound metal and the metal dissolved in the nominally 5 grams of water per gram of pulp that remains with the pulp in the mat. The variation in concentration that produces local maxima at cycles 2, 6, and 9 are probably due to variations in the final pulp consistency since this was not controlled for the final stage. Ignoring the variation, it appears that all metal concentrations continue to rise through the ten cycles, but there may be a decrease in slope around the 5th cycle.

Simple Model: Excel Spreadsheet Model of All Cycles

The Excel spreadsheet model consists of three macros that iteratively solve the partition equation for metals relative to pH, competition between monovalent and divalent metals, and competition between metals of like valency. The input for each of the macros included, the selectivity coefficient for the cation pair, the pulp acid content, the Debye Hückel parameters for estimating the activity coefficient of each metal in the pair, the total input metal concentration of the two metals in the pair, and the estimated ionic strength. Ionic strength was estimated by summing the total soluble cation concentration terms only; the concentrations of monovalent and divalent anions was assumed to be similar to the concentrations of monovalent and divalent cations. Although the concentrations of sulfate and chloride can be estimated with reasonable accuracy, the concentrations of organic acids and carbonate as byproducts of bleaching are unknown. This assumption does not have a significant impact on the model results. The output value from each macro is the fraction of acid sites occupied (or neutralized) by one of the two metals.

The competition for acid sites between cation pairs was solved iteratively in the spreadsheet as follows:

- 1) Calcium was selected as the common cation used in solution of the partition macro for each of the other cations.
- 2) The input ion exchange concentration to each macro was the concentration of acid groups involved in the competition between calcium and the other cation of the cation pair.
 - a) The output value of the macro, F_M , is therefore $[CaR_2]/([CaR_2]+[M_1R_x])$, where the square brackets indicate the fraction of acid sites occupied (neutralized) by each of the two cations and R_x is the appropriate stoichiometry for the competing cation, 1 for Na⁺ and H⁺, 2 for Mg²⁺, Ba²⁺, and Mn²⁺.
- 3) The new estimate for the fraction of total acid sites occupied by calcium $[CaR_2]$ was determined by summing the reciprocals of the charge fraction for all cation pairs. Since the sum of the charge fractions of H⁺, Na⁺, Mg²⁺, Ba²⁺, Mn²⁺, and Ca²⁺ is by definition 1, this simplifies to:

$$\sum 1/F_M = (1 + 4[CaR_2])/[CaR_2]$$

where the summation is carried out for cation competition between calcium and H⁺, Na⁺, Mg²⁺, Ba²⁺, and Mn²⁺. $[CaR_2]/F_M \times [a_M]$ (where $[a_M]$ is the concentration of acid sites) then provides a new estimate of acid sites in competition between Ca²⁺ and each of the other cations.

The spreadsheet only modeled the washing process. All added chemicals were considered as inputs to the washer vat, and the adsorption equilibrium was calculated based on the pH and metals

concentration of the washer vat. The assumption contained in this method is that the retention time on the washer is not sufficient to make significant progress towards the new equilibrium at the pH and filtrate metals concentrations of the wash water. Soluble complex formation such as $\text{Ca}(\text{OH})^+$ and precipitation such as BaSO_4 were not considered in the model. These limitations can lead to significant errors in the model, but most significant would be the failure to consider the partition of precipitates between the pulp mat and filtrate. This simplified model should underestimate the concentration on pulp of cations that experience significant precipitation reactions in the experiment and should overestimate the concentration on pulp of cations that participate in significant complex formation reactions in the experiment. These issues are addressed in the detailed model of the 10th cycle using the OLI software (*vide infra*).

The direct countercurrent bleach filtrate recycle experiment was carried out at a wash liquor ratio (R_w) of 1.2 and an assumed displacement ratio (d_r) of 0.8. The dilution vat pulp consistency was 3.0 wt% (pulp solids concentration $C_{p,v}$ of 0.031 kg pulp/kg liquor), and the filtered pulp mat consistency was 12.0 wt% (pulp solids concentration $C_{p,f}$ of 0.136 kg pulp/kg liquor). Filtrate amounts were calculated from these parameters, assuming 75 g dry pulp solids. The 75 g pulp was diluted to 3.0 wt% consistency in 2425 g dilution liquor, which includes 2315 g dilution filtrate from internal recycle and 110 g liquor carryover from the previous washing stage. A total of 660 g wash liquor was added to the process during displacement washing. Specifically, 440 g of the wash liquor was retained in the final pulp mat, whereas 220 g passed through the pulp into the filtrate tank. The 220 g wash liquor that passed through the pulp was mixed with 2315 g dilution liquor recycle in the filtrate tank to provide a total filtrate of 2535 g. Consequently, 220 g of the fresh 660 g wash liquor added to the process was carried back counter-currently through the process. Finally, there was 550 g liquor in the final pulp mat at 12 wt% consistency, including 110 g of dilution vat liquor carryover and 440 g of wash liquor.

Results of the Spreadsheet Model:

The estimated and analyzed sodium and calcium concentration in D_0 filtrate is given in *Figure 7* and for magnesium, manganese, and barium in *Figure 8*. The model accurately estimates the concentration of all five cations in the D_0 filtrate. One assumption was needed to match the estimated filtrate to the analytical results. Calcium enters the bleach plant as carbonate and does not participate in the pulp adsorption equilibrium until the carbonate dissolves in the D_0 stage. A tunable “washable calcium” parameter was used to optimize the estimates. The best fit model gave about 35% of the calcium as washable. This could either be the amount that dissolves during the washing process with the acidic D_0 filtrate, or the amount of particulate calcium carbonate that was displaced from the fibers in the dilution/thickening and displacement washing process.

The concentration maximum that occurs in the second cycle for magnesium and manganese is observed in the model, as is the change in slope of the sodium buildup after the third cycle. A significant deviation between the soluble barium analysis and model estimate is observed after the 7th cycle. This error is consistent with formation and physical entrapment of barium sulfate precipitates.

The estimated Na^+ and Ca^{2+} concentrations on D_1 pulp are within the scatter of the analytical data (*Figure 9*), but the model underestimates the concentration of Mg^{2+} and Ba^{2+} on D_1 pulp by about 50% (*Figure 10*). This error could also be due to precipitation of BaSO_4 in D_0 and precipitation of $\text{Mg}(\text{OH})_2$ and $\text{Mn}(\text{OH})_2$ in EP carrying the entrapped particles with the fiber into D_1 .

DETAILED MODEL, OLI ANALYSIS

OLI Process Model

The laboratory experiment was simulated on OLI Systems ESP software version 6.0 (Jan. 1, 1998 release, Morris Plains, NJ). The OLI-ESP software is an “equilibrium calculator” for aqueous electrolyte speciation that is integrated into a material and energy balance simulator. The OLI database contains over 2000 compounds and uses a speciation generator to determine permutations of all possible ionic and neutral species resulting from interactions of H^+ , Na^+ , Ca^{+2} , Ba^{+2} , Mg^{+2} and Mn^{+2} , cations with Cl^- , OH^- , CO_3^{-2} , SO_4^{-2} , and $\text{C}_2\text{O}_4^{-2}$ anions in the wash liquors.

NPE metal concentration data were available for the starting pulp, the EP-stage pulp, and the D_0 , EP, and D_1 filtrates. To facilitate comparison of model predictions to available data, the OD(EP) portion

of the experiment was modeled using the OLI-ESP software. The metal concentration measurements for the starting pulp and the D₁ filtrate were used as process material balance inputs.

In the development of the OLI block diagram for the OD(EP) portion of the experiment, the displacement-washing step from the previous bleach stage was lumped into the dilution-washing step of the next bleaching stage. Basically, the wash liquor designated for addition to the final mat was routed to the dilution vat MIX block of the next stage. This consolidation of process streams had no effect on thermodynamic equilibrium in the dilution vat or the filtrate tanks but considerably simplified the process calculations. The OLI process block diagram is presented in *Figure 11*.

Equilibrium calculations were performed in the MIX blocks, whereas solids separation and filtrate recycle were carried out in SEP and SPLT blocks respectively. The SEP block was set to entrainment mode, with the dissolved liquids to solids ratio in each SEP block defined as:

$$\frac{\text{dilution vat liquid retained in mat}}{\text{pulp solids}} = \frac{110 \text{ g}}{75 \text{ g}} = \frac{1 - d_r}{C_{p,f}} = 1.4667 \quad (3)$$

Equation (3) applied to streams *F5*, *F10*, and *F14* in *Figure 11*. From manipulation of material balance relationships, the split fraction for the filtrate stream in each SPLT block was defined as

$$\frac{\text{filtrate internal recycle to dilution vat}}{\text{total filtrate}} = \frac{2315 \text{ g}}{2535 \text{ g}} = \frac{1 - \frac{C_{p,v}}{C_{p,f}}(1 - d_r)}{1 + \frac{C_{p,v}}{C_{p,f}}(R_w - 1)} = 0.9132 \quad (4)$$

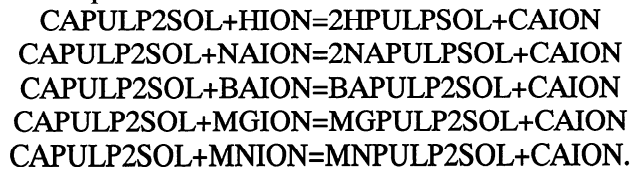
Equation (4) applied to split streams *F7* and *F12* in *Figure 11*.

Addition of the ion exchange reactions for metal ions with pulp in the OLI-ESP software requires the setup of a SORPTION database, where each metal-pulp complex must be defined as a unique solid species. The critical item of input data is the molecular weight of a given metal pulp complex, which is calculated by

$$M_w(M_i^{+z} - \text{pulp}_z) = \frac{v_i}{q_T} - \frac{v_i M_{w,H}}{v_H} + M_{w,i} \quad (5)$$

where $M_{w,i}$ is the molecular weight of the particular NPE species and $M_{w,H}$ is the molecular weight of hydrogen, v_i is the equivalents of ion exchange sites per mole of the metal ion (equal to 1.0 for monovalent metal ions or 2.0 for divalent metal ions), and q_T is the carboxylate site concentration of the pulp (meq/kg pulp). Although the carboxylate site concentration on pulp can change during bleaching, it was assumed to be constant at 87 mmol/kg pulp for each bleaching stage.

Finally, the ion exchange reactions for H⁺, Na⁺, Ba⁺², Mg⁺², and Mn⁺² for displacement of Ca-exchanged pulp, written in the OLI input format are:



Process Input Parameters for OLI Process Model

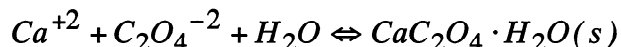
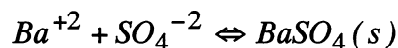
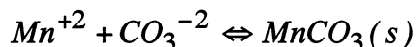
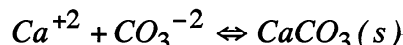
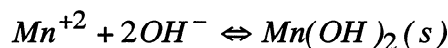
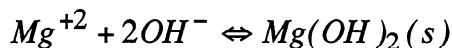
Measured concentrations of NPE metals in the inlet pulp suspension (stream *F1*) and D₁ filtrate (stream *F16*) at cycle 10 are provided in *Tables 6* and *7*, respectively. The ICP analyses did not provide information on anionic species associated with pulp and filtrate samples. However, the OLI software requires the specification of molecular species as chemical inputs. It was assumed that starting pulp was completely in the Na-exchanged form (NAPULPSOL), where the carboxylate functional group concentration on the pulp was 87 meq/kg. The CaSO₄ input was estimated from the ICP sulfur analysis. The balances of Na, Ca, Mg, Mn, and Ba loaded on the pulp were assumed to be in the form of carbonate salts. The measured metals in the D₁ filtrate were taken as their soluble chloride salts, and the sulfuric

acid carryover was estimated from the ICP sulfur analysis. No carbonate was assumed to be present in the D_1 filtrate.

Known quantities of input bleach chemicals from the experiment were added directly to the D_0 and EP dilution vat MIX blocks (streams $F6$, $F11$), as shown in *Table 8*. Consumption of bleach chemicals and formation of chemical byproducts of bleaching were not predicted by the OLI model. Consequently, reaction-driven dissociation of ClO_2 was not predicted, so ClO_2 was replaced with the molar equivalent amount of Cl_2 . The Cl_2 was speciated but not consumed. Also, formation of oxalate during D-stage bleaching was approximated by adding oxalic acid directly to the dilution vat (stream $F6$) in the amount of 12.6 mmol/kg pulp for the D_0 stage. Oxalic acid was added directly to the D_1 filtrate (stream $F16$) at 0.11 mM. These oxalic acid concentrations were estimated from oxalic acid assays of the D_0 and D_1 filtrates from the laboratory experiment. All process equilibrium calculations were carried out isothermally at a temperature of 50° C and, pressure of 1.0 atm. Vapor phase equilibrium calculations were turned off.

Model Simulation Results

Based on the process input given in *Tables 6 to 8*, OLI model results were compared to experimental data. The OLI aqueous speciation generator predicted the formation of 32 molecular species, as shown in *Table 9*. Based on the chemical input species and their compositions, the OLI-ESP speciation generator predicted the following precipitation reactions:



Neither the carbonate precipitates $BaCO_3$, $MgCO_3$, and $MnCO_3$ nor the hydroxide precipitates $Ba(OH)_2$ and $Ca(OH)_2$ were predicted because these molecular species were present at concentrations below their solubility limits or their formation was not thermodynamically favored at the process conditions.

Recall that the ICP analyses determined the elemental composition of a given pulp solid or filtrate sample. Therefore, to facilitate comparison of model predictions to data, the OLI-predicted molecular species for a common NPE metal within a given phase were lumped together. Furthermore, all precipitates were assumed to be associated with the pulp solid phase. On this basis, the predicted and measured NPE metal concentration profile in the D_0 stage dilution vat for cycle 10 are compared in *Figure 12*, and the predicted NPE metal concentration profile in the EP stage dilution vat pulp is presented in *Figure 13*. The predicted vs. measured soluble metal concentrations in the D_0 and EP filtrate tanks are presented in *Figures 14 and 15*, respectively. The simulation results confirmed that metals move from the pulp to liquor in acidic D-stages and from the liquor back to the pulp in the alkaline E-stage. Furthermore, a significant fraction of the metals loaded on the pulp were precipitates, not adsorbed species. At pH ~3, the adsorbed hydrogen occupied 88% of the available acid sites, and the metal loading on the pulp (*Figure 12*) included 216 mg/kg pulp of adsorbed metals and 517 mg/kg pulp of precipitated metals, for a total loading of 733 mg/kg pulp. The predicted precipitates present were barium sulfate $BaSO_4(s)$ and calcium oxalate monohydrate ($CaC_2O_4 \cdot H_2O(s)$). The predicted concentrations of Mg and Mn adsorbed on the pulp were negligible, below 1.0 mg/kg pulp.

In the EP stage, at pH ~10.5, 99.5% of the carboxylate sites on the pulp were occupied by Na (70.2 %) and Ca (29.3 mol %). The predicted metal loading on the pulp included 1915 mg/kg pulp of adsorbed metals and 958 mg/kg pulp of precipitated metals, for a total loading of 2873 mg/kg pulp. In comparison, the total analyzed NPE loading on the pulp was 3293 mg/kg pulp. The predicted concentration of Ba, Mg, and Mn adsorbed on the pulp were all below 1.0 mg/kg pulp. Carryover of sulfate and oxalate from the D_1 filtrate wash promoted the formation of $BaSO_4(s)$ and $CaC_2O_4 \cdot H_2O(s)$.

All Ba loaded on the pulp was BaSO₄ (s). Furthermore, alkaline conditions promoted the formation of carbonate and hydroxide precipitates, including CaCO₃ (s), Mg(OH)₂ (s), and Mn(OH)₂ (s). As shown in *Figure 13*, the predicted NPE profile in the pulp generally agreed with the measured NPE profile, and each metal within the NPE metal profile was predicted at the correct order of magnitude. With the exception of Mg, differences between model and data were generally less than 30%, which is acceptable considering the complexity of both the model and the experiment.

The predicted soluble NPE profiles in the D₀ and EP filtrates (*Figures 14 and 15* respectively) reflect the H⁺ promoted displacement of adsorbed metals at low pH and the re-adsorption and precipitation of metals on the pulp at high pH. Of particular note is the large swing in Ca concentration, from 395 mg Ca/L in the D₀ stage filtrate down to 26 mg Ca/L in the EP stage filtrate. Next to H⁺, Ca⁺² is the most strongly bound cation on the pulp. Therefore, at low H⁺ concentration, Ca⁺² will readily adsorb onto the pulp, which lowers its concentration in the filtrate. The predicted NPE profile in the filtrates generally agreed with the measured NPE profile. However, there were two differences. First, the model predicted that the total soluble Ba concentration in the EP filtrate was 0.053 mg Ba/L at 50° C, vs. a measured D₀ filtrate concentration of 0.46 mg Ba/L. This result suggests that some of the Ba precipitates were suspended in the filtrate obtained from the experiment. Second, the predicted Na concentration was much higher than observed, suggesting that the Na loading on the pulp was under predicted in the D₀ stage. However, this point was not verified, as the NPE profile of the D₀ vat pulp was not in the experiment.

Finally, comparison of the filtrate compositions in *Table 9* reveal the complex patterns of metal ion buildup in the filtrates as the wash water was transferred counter-currently from the D₁ to the EP and D₀ stages. Significant accumulations of Ca and Mn are predicted. Total soluble Ca increased from 2.0·10⁻³ to 9.9·10⁻³ M from D₁ to D₀, whereas total soluble Mn increased from 6·10⁻⁵ to 2.6·10⁻⁴ M. In contrast, total soluble Ba decreased from 3·10⁻⁶ M to 3·10⁻⁷ M as the result of sulfate precipitation.

CONCLUSIONS:

The buildup of trace metals was followed in a batch-wise bleach filtrate recycle experiment that simulated a mill with an OD(EP)D bleach sequence and direct countercurrent use of wash filtrates. Calcium and sodium were observed to build up in the D₀ filtrate through all ten cycles and show no evidence of reaching a process equilibrium. In contrast, the trace metals present at lower concentration, magnesium, barium, and manganese, all reached equilibrium after about 5 cycles. This may be due to precipitation of BaSO₄ in the first chlorine dioxide stage and Mn(OH)₂ and Mg(OH)₂ in the extraction stage. These precipitates limit the concentration of these cations in the EP filtrate. All metals appear to continue accumulating in the D₁ pulp through all ten cycles, although this is hard to judge because of considerable scatter in the data. A simple model of the batch recycle experiment can predict the buildup with reasonable accuracy but underestimates some trace metal concentration by as much as 50%. Checking the soluble metal estimates, predicted sulfate concentration, and analyzed oxalate concentration against the solubility products for barium sulfate and calcium oxalate suggests that these ions should precipitate in the D₀ vat and filtrates. A detailed OLI process model of the tenth cycle provides a slightly closer match of predicted metal content to observe. Precipitation of BaSO₄, CaC₂O₄·H₂O, CaCO₃, Mg(OH)₂, and Mn(OH)₂ were all predicted by the OLI software. No precipitates were actually observed in the experimental work but these would be expected to be obscured by fiber and collected by the filter paper. Confirmation of the presence of these precipitates and partitioning of precipitates between the pulp mat and filtrates remain a significant problems in developing and validating NPE process models.

ACKNOWLEDGEMENTS

This research was partially supported by the U.S. Department of Energy Agenda 2020 Program under contract DE-FC07-961D13441 and the Georgia Traditional Industries Program in Pulp and Paper under grants MP1-FY99 and MP4-FY99. Research support was also provided by the member companies of the Institute of Paper Science and Technology (IPST), Atlanta, GA. GLR kindly acknowledges IPST for partial salary support to complete this work during his sabbatical leave. Portions of this work were used by A. Puckett in partial fulfillment of the requirements for the Masters of Science degree at the Institute of Paper Science and Technology.

Figure Legends

Figure 1. Distribution plots for exchange of H^+ and Na^+ with Ca^{+2} on pulp. The x-axis intercept is $\log K$, and the slope is $1/n$.

Figure 2. Distribution plots for exchange of Ba^{+2} , Mg^{+2} , and Mn^{+2} with Ca^{+2} on pulp. The x-axis intercept is $\log K$, and the slope is $1/n$.

Figure 3. Buildup of sodium and calcium in the D_0 filtrate for the ten cycles of the bleach filtrate recycle experiment.

Figure 4. Buildup of magnesium, barium, and manganese in the D_0 filtrate.

Figure 5. Sodium and calcium analysis of D_1 pulp for all ten cycles of the bleach filtrate recycle experiment.

Figure 6. Buildup of magnesium, barium, and manganese on D_1 pulp.

Figure 7. Spreadsheet model of the buildup of sodium and calcium in the D_0 filtrate.

Figure 8. Spreadsheet model of the buildup of magnesium, barium, and manganese in the D_0 filtrate.

Figure 9. Spreadsheet model of the buildup of sodium and calcium on the D_1 pulp.

Figure 10. Spreadsheet model of the buildup of magnesium, barium, and manganese in D_1 pulp.

Figure 11. Simplified OLI-ESP process block diagram for the OD(EP) stages of the experiment.

Figure 12. Adsorbed and total NPE metal concentrations on the D_0 stage dilution vat pulp predicted by the OLI model: (a) log scale, (b) linear scale. The precipitate concentration on the pulp is the difference between the total and adsorbed concentration.

Figure 13. Adsorbed and total NPE metal concentrations on the EP stage, dilution-vat pulp: comparison of OLI model predictions and ICP data: (a) log scale, (b) linear scale. The precipitate concentration on the pulp is the difference between the total and adsorbed concentration.

Figure 14. Comparison of predicted vs. measured NPE metal profiles in the D_0 filtrate: (a) log scale, (b) linear scale.

Figure 15. Comparison of predicted vs. measured NPE metal profiles in the EP filtrate: (a) log scale, (b) linear scale.

REFERENCES

1. Ohlsson, A. and Rydin, S., "Washing of Pulps, Part 2. Sorption of Na, Mg and Ca on Kraft Pulp", *Svensk Papperstidning*, **78**(15): 549-552 (1975).
2. Bryant, P.S. and Edwards, L.L., "Cation Exchange of Metals on Kraft Pulp", *J. Pulp and Paper Sci.*, **22**(1): 37-42 (1996).
3. Caulkins, D. and Wildman, J., "Changes in Paper Process Causing Problems in Controlling Deposits", *Pulp and Paper*, **62**(6): 89-93 (1988).
4. Dexter, R.J. and Wang, X.H., "The formation and control of bleach plant scale as a result of water minimization", Proceedings, 1998 Tappi Pulping Conference, pp. 1341-1347 (1998).
5. Bryant, P., Samuelsson, Å., and Basta, J., "Minimizing BaSO₄ Scale Formation in ECF Bleach Plants" Proceedings, 1997 Tappi Minimum Effluent Mill Symposium, pp. 205-210 (1997).
6. Sjöström, E., Janson, J., Haglund, P., and Enström, B., "The Acidic Groups in Wood and Pulp as Measured by Ion Exchange", *J Polymer Sci. C*, (11): 221-241 (1965).
7. Rosen, A., "Adsorption of Sodium Ions on Kraft Pulp Fibers During Washing", *Tappi J.*, **58**(9): 156-161 (1975).
8. Helfferich, F.G., Ion Exchange, Dover Publications, Inc., New York, pp. 134-135(1995).
9. Lange's Handbook of Chemistry, 14th ed., Dean, J.A. ed., McGraw Hill, Inc, New York, pp. 8.13-8.15 (1992).
10. Fernandes Diniz, J.M.B., "Application of Chemical Equilibrium to Wood Pulps", *Holsforshung*, **50**(5): 429-433 (1996).
11. Pulp samples digested using an adaptation of Solid Waste 846, method 3050. This procedure uses a mixture of nitric acid, hydrochloric acid and hydrogen peroxide to digest solid materials.
12. Wilson, K., "Determination of Carboxyl Groups in Cellulose", *Svensk Papperstidning*, **69**(11): 386-390(1966).
13. Helfferich, F., *ibid.*, pp. 153-154.
14. Helfferich, F., *ibid.*, pp. 185.
15. Helfferich, F., *ibid.*, pp. 166.
16. Laine, J., Lövgren, L., Stenius, P. and Sjöberg, S., "Potentiometric Titration of Unbleached Kraft Cellulose Fibre Surfaces", *Colloids and Surfaces*, **88**: 277-287 (1994).
17. Lange's Handbook of Chemistry, *ibid.*, pp. 8.2-8.5.

Table 1. Binary equilibrium constants for ion exchange of selected cations on pulp at 25°C.

K Definition	$\log K$ +/- S.E. (95%)	K	n +/- S.E. (95%)	Theory n
$K^{Ca/H}$	-2.377 +/- 0.092	0.00420	0.61 +/- 0.02	2
$K^{Ca/Na}$	2.739 +/- 0.423	548.0	1.72 +/- 0.20	2
$K^{Ca/Mg}$	0.610 +/- 0.101	4.07	1.12 +/- 0.13	1
$K^{Mg/Ba}$	0.236 +/- 0.049	1.72	1.02 +/- 0.06	1
$K^{Mg/Mn}$	0.373 +/- 0.187	2.36	1.15 +/- 0.22	1

Table 2. Binary equilibrium constants scaled to Ca-exchanged basis using the Triangle Rule.

Scaled K	Probe Ion	Form of Pulp	K Value OLI	K Value Spreadsheet
$K_{H2} = 1 / K_{2H}$	H ⁺ (H)	Ca ⁺² (2)	238.0	2 (n=1)
$K_{12} = 1 / K_{21}$	Na ⁺ (1)	Ca ⁺²	0.002	0.9 (n=2)
$K_{32} = 1 / (K_{43} K_{24})$	Ba ⁺² (3)	Ca ⁺²	0.143	0.43
$K_{42} = 1 / K_{24}$	Mg ⁺² (4)	Ca ⁺²	0.246	0.43
$K_{52} = 1 / (K_{45} K_{24})$	Mn ⁺² (5)	Ca ⁺²	0.104	0.67

Table 3. Trace metal analysis of the two starting pulps used in the laboratory bleaching filtrate recycle experiments.

Metal (ppm)	Pulp 1 (Cycles 1 & 2)	Pulp 2 (Cycles 3-10)
Kappa	12.5	9.8
Viscosity	15.9	18.9
Na	499	2350
Ca	1600	2360
Mg	472	188
Ba	15.8	29.9
Mn	132	52.6

Table 4. Conditions used in the laboratory bleaching.

	D ₀	EP	D ₁
Pulp (ODg)	75	75	65
Consistency (%)	3.0	12	12
Temperature (°C)	50	70	70
Time (hrs)	0.5	1.0	3.0
ClO ₂ (%)	1.0		1.2
NaOH		To pH > 10.5	None
H ₂ O ₂ (%)		0.3	
H ₂ SO ₄	To pH 3.0		None
Vat csc. (%)	3.0	3.0	3.0
Mat csc (%)	12.0	12.0	12.0
Wash volume (ml)	660	660	580

Table 5. Bleaching results

Cycle	Extracted Kappa	Final ISO Brightness	Final Viscosity (mPa•sec)
1	4.8	81.6	10.0
2	4.9	79.6	7.3
3	5.2	84.0	12.2
4	4.9	84.7	12.0
5	4.8	83.6	12.5
6	5.3	83.7	10.8
7	5.5	84.6	13.9
8	4.9	84.7	13.9
9	5.4	84.4	11.5
10	5.2	84.8	13.5

Table 6. Chemical inputs for OLI process block stream F1. Functional group content of pulp set at 87 mmol/kg pulp, 74.3 g H-exchanged pulp input basis (75.02 g total solids).

Species	Mol. Wt.		ICP Analysis (per kg pulp)			OLI Input Stream F1		
	g/mol	g/mol pulp	mg/kg	mmol/kg	meq/kg	Compound	Molality	g/sec
Ba-Pulp	137.3	23123.8	29.9	0.218	0.000	BAPULP2SOL	0.000E+00	0.0000
BaCO ₃	197.3				0.436	BACO3	7.338E-06	0.0032
Ca-Pulp	40.0	23026.5	2350.0	58.750	0.000	CAPULP2SOL	0.000E+00	0.0000
CaCO ₃	100.0				100.000	CACO3	1.685E-03	0.3715
CaSO ₄	136.0				17.500	CASO4	2.948E-04	0.0884
Mg-Pulp	24.3	23010.8	188.0	7.737	0.000	MGPULP2SOL	0.000E+00	0.0000
MgCO ₃	84.3				15.473	MGCO3	2.607E-04	0.0485
Mn-Pulp	54.9	23041.4	52.6	0.958	0.000	MNPULP2SOL	0.000E+00	0.0000
MnCO ₃	114.9				1.916	MNCO3	3.228E-05	0.0082
Na-Pulp	23.0	11516.3	2360.0	102.609	87.000	NAPULPSOL	2.932E-03	74.4422
Na ₂ CO ₃	106.0				15.609	NA2CO3	2.630E-04	0.0615
						H2O	55.509	2205.0000
Total			4980.50	170.27	237.93	TOTSOL		75.0234

Table 7. Chemical inputs for OLI process block diagram stream F16.

Element	ICP of D_1 Filtrate Mg/kg filtrate	OLI Input Stream F16		
		Compound	Molality	g/sec
Mn	3.41	MNCL2	6.211E-05	1.720E-03
Ba	1.44	BACL2	1.049E-05	4.806E-04
Na	227.00	NACL	9.870E-03	1.270E-01
Mg	12.40	MGCL2	5.103E-04	1.070E-02
Ca	81.30	CACL2	2.033E-03	4.963E-02
S	9.09	H2SO4	2.841E-04	6.125E-03
		OXALIC	1.111E-04	2.200E-03
		H2O	55.509	220.0

Table 8. Bleach chemical inputs for OLI process block diagram.

Compound	OLI Species	Input Stream	g/sec
H ₂ SO ₄	H2SO4	F6	0.294
Cl ₂	CL2	F6	0.394
H ₂ C ₂ O ₄	OXALIC	F6	0.085
NaOH	NAOH	F11	0.48
		F1	0.04

Table 9. Predicted molecular species compositions in filtrates.

No.	Molecular Species	OLI Predicted Filtrate Composition (Molality)		
		D _o	E _o	D ₁
1	BaCl ₂	1.73E-07	3.04E-07	2.75E-06
2	BaC ₂ O ₄	1.61E-12	4.42E-11	7.08E-11
3	BaCO ₃	0.00E+00	8.42E-10	0.00E+00
4	BaSO ₄	1.30E-07	1.30E-07	1.31E-07
5	CaC ₂ O ₄	1.64E-05	1.64E-05	1.09E-05
6	CaC ₂ O ₄ ·H ₂ O	0.00E+00	0.00E+00	0.00E+00
7	Ca(HC ₂ O ₄) ₂	4.91E-11	0.00E+00	8.27E-11
8	CaCl ₂	8.28E-03	5.55E-04	2.00E-03
9	CaCO ₃	7.65E-12	6.93E-06	0.00E+00
10	CaSO ₄	1.57E-03	5.76E-05	2.38E-05
11	Cl ₂	2.83E-04	0.00E+00	0.00E+00
12	CO ₂	5.43E-03	8.02E-11	0.00E+00
13	H ₂ O	5.55E+01	5.55E+01	5.55E+01
14	HCl	3.75E-11	0.00E+00	6.22E-04
15	HClO	2.09E-02	6.98E-03	0.00E+00
16	MgC ₂ O ₄	1.29E-05	4.65E-07	3.66E-05
17	MgCl ₂	4.50E-04	1.39E-06	4.70E-04
18	Mg(OH) ₂	0.00E+00	0.00E+00	0.00E+00
19	MgSO ₄	6.32E-05	8.31E-08	4.10E-06
20	MnC ₂ O ₄	9.06E-05	7.57E-07	4.13E-05
21	MnCl ₂	1.26E-04	7.85E-07	2.04E-05
22	Mn(OH) ₂	0.00E+00	1.22E-07	0.00E+00
23	MnSO ₄	4.30E-05	1.31E-08	4.49E-07
24	Na ₂ C ₂ O ₄	1.28E-05	2.38E-05	0.00E+00
25	Na ₂ SO ₄	5.81E-03	0.00E+00	0.00E+00
26	Na ₃ H(SO ₄) ₂	1.14E-03	1.66E-03	1.24E-04
27	Na ₆ (SO ₄) ₂ CO ₃	6.82E-06	2.02E-05	0.00E+00
28	NaCl	1.19E-02	1.83E-02	9.50E-03
29	NaHCO ₃	7.87E-08	4.60E-08	0.00E+00
30	NaOH	0.00E+00	1.19E-02	0.00E+00
31	H ₂ C ₂ O ₄	9.09E-08	0.00E+00	2.23E-05
32	SO ₃	0.00E+00	0.00E+00	1.68E-10

Fig. 1

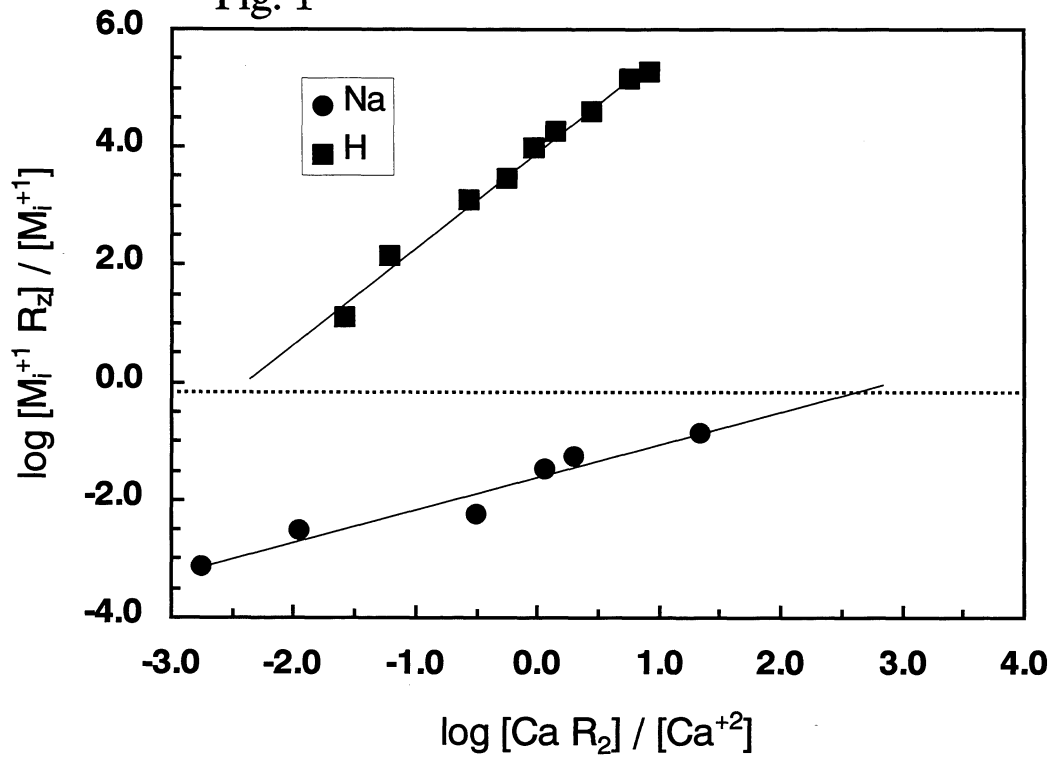


Fig. 2

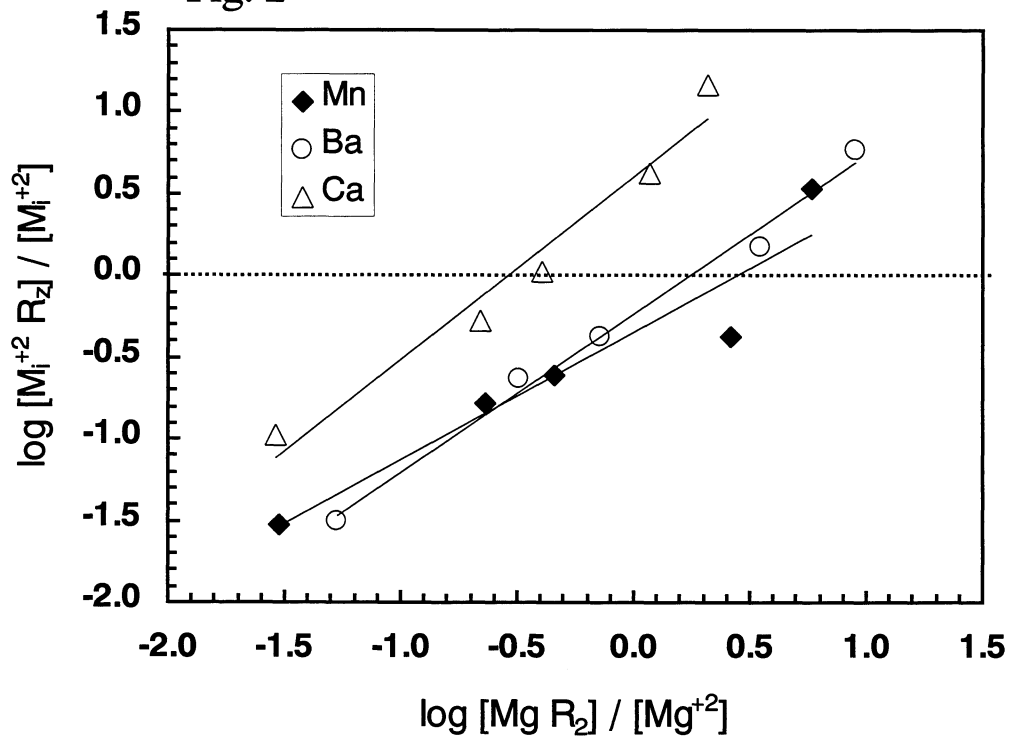


Fig. 3

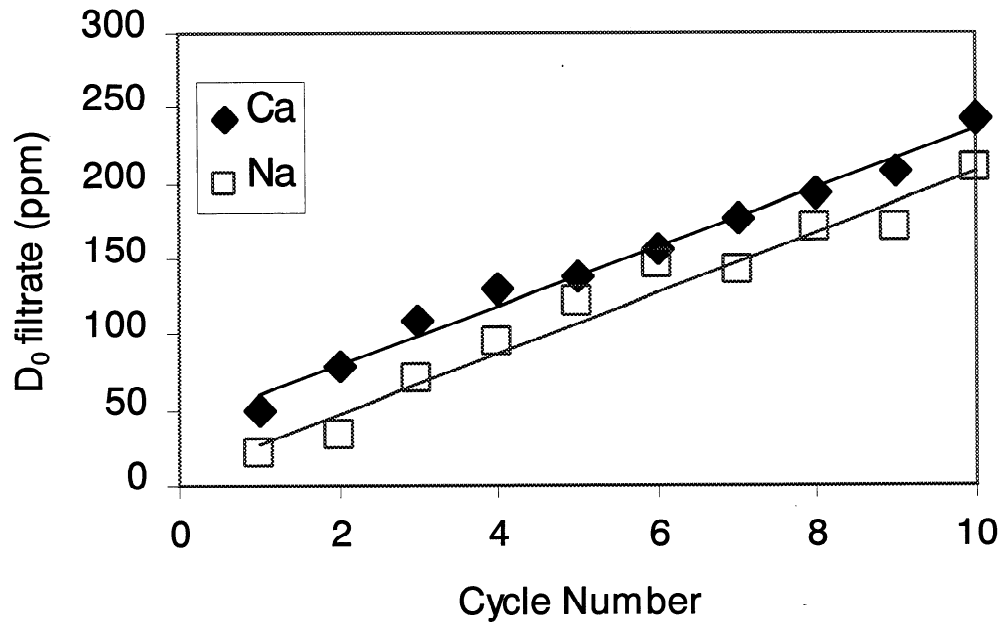


Fig. 4

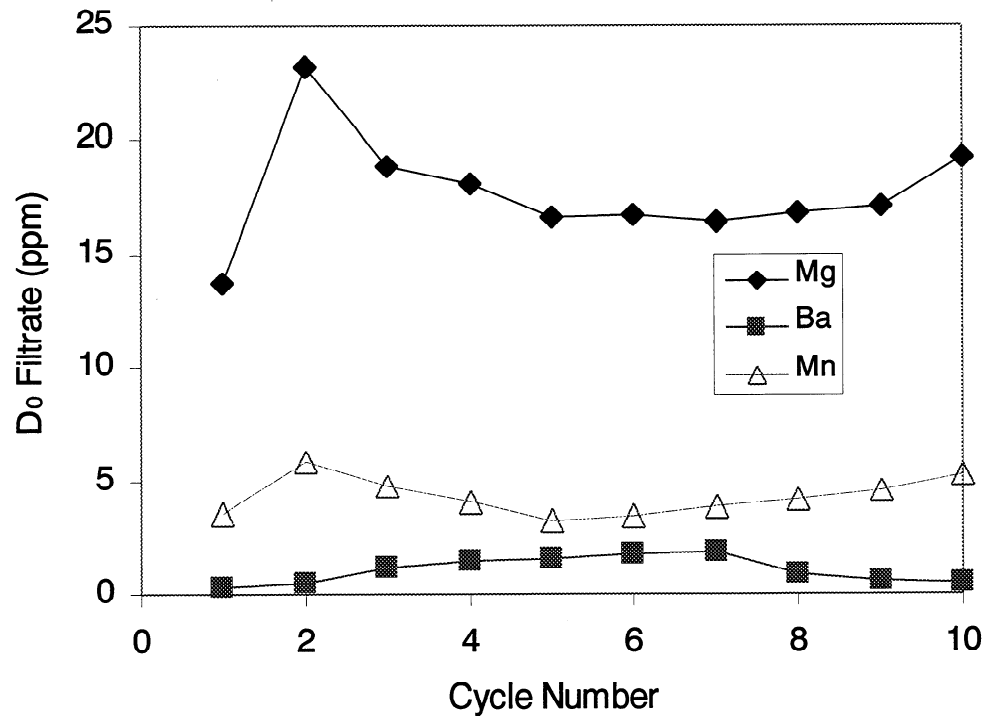


Fig. 5

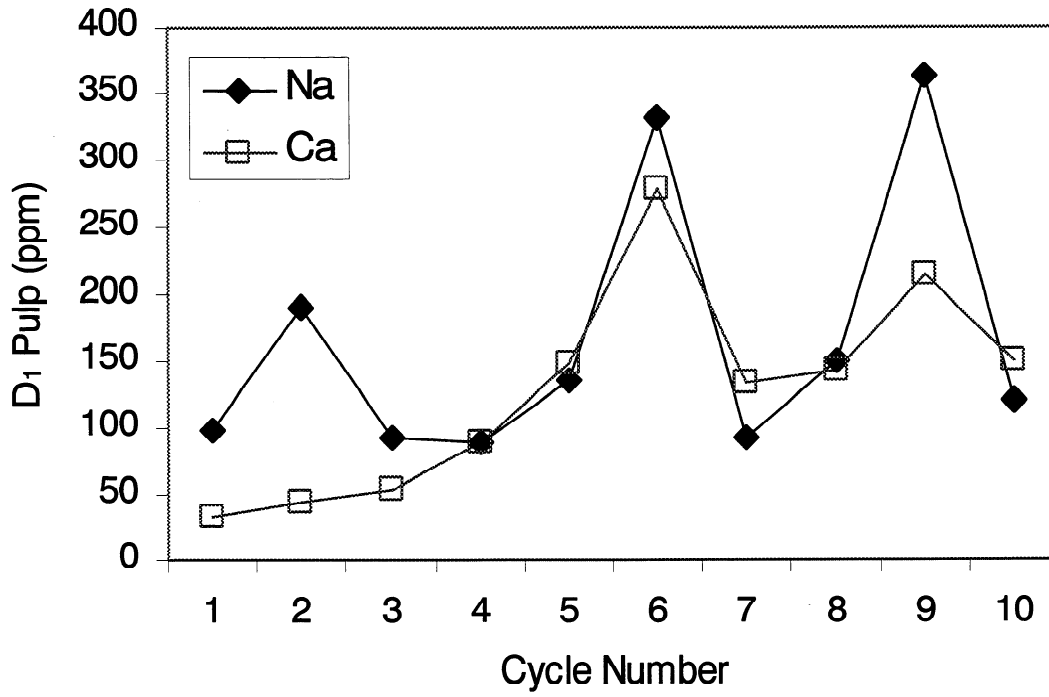


Fig. 6

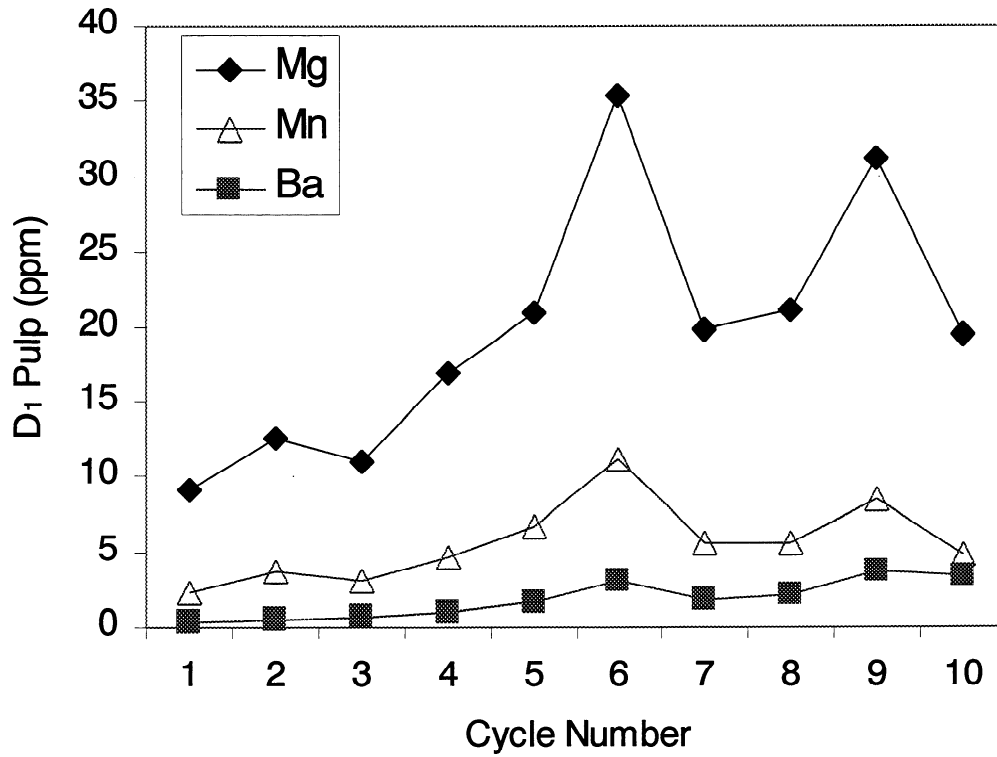


Fig. 7

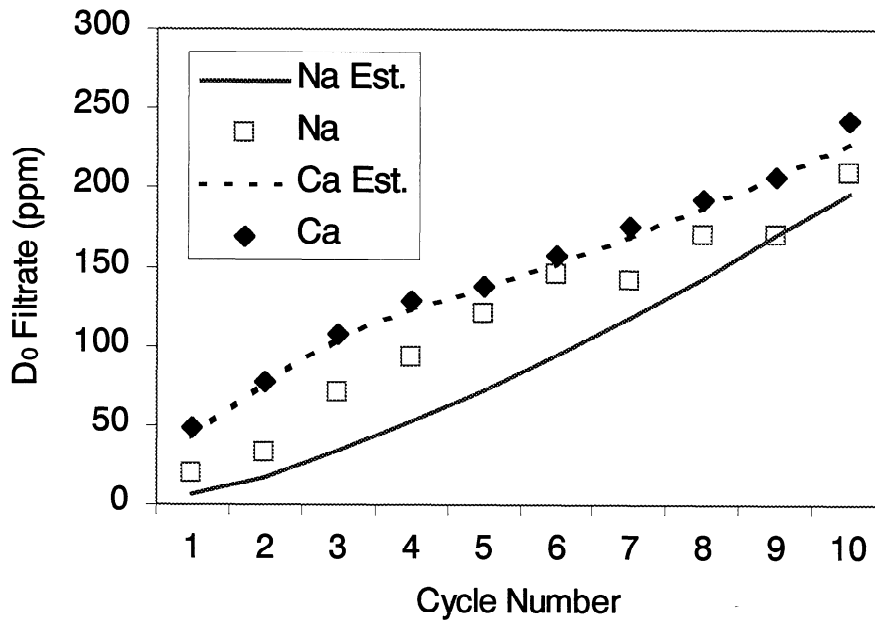


Fig. 8

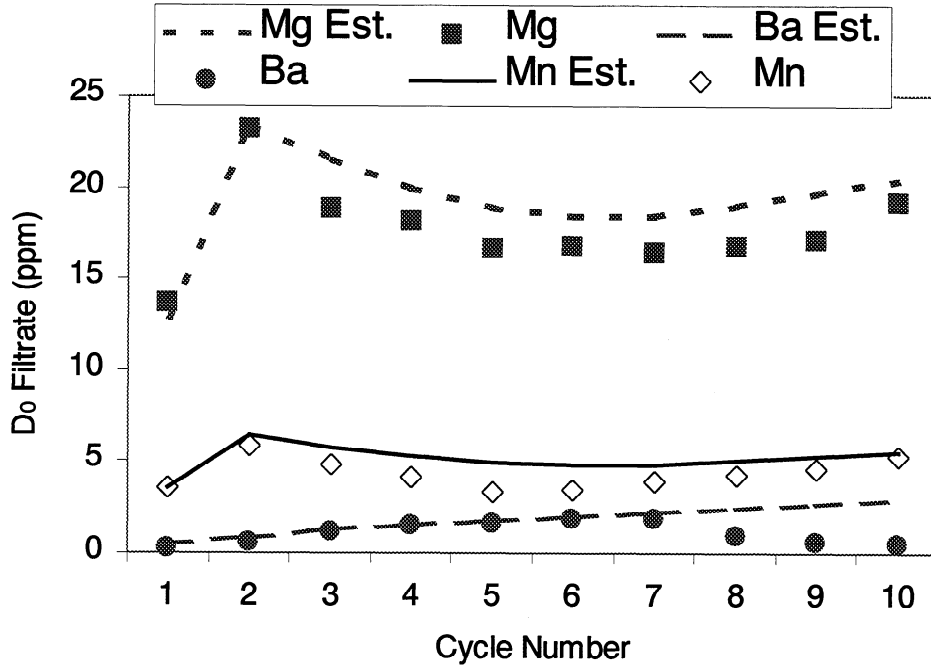


Fig. 9

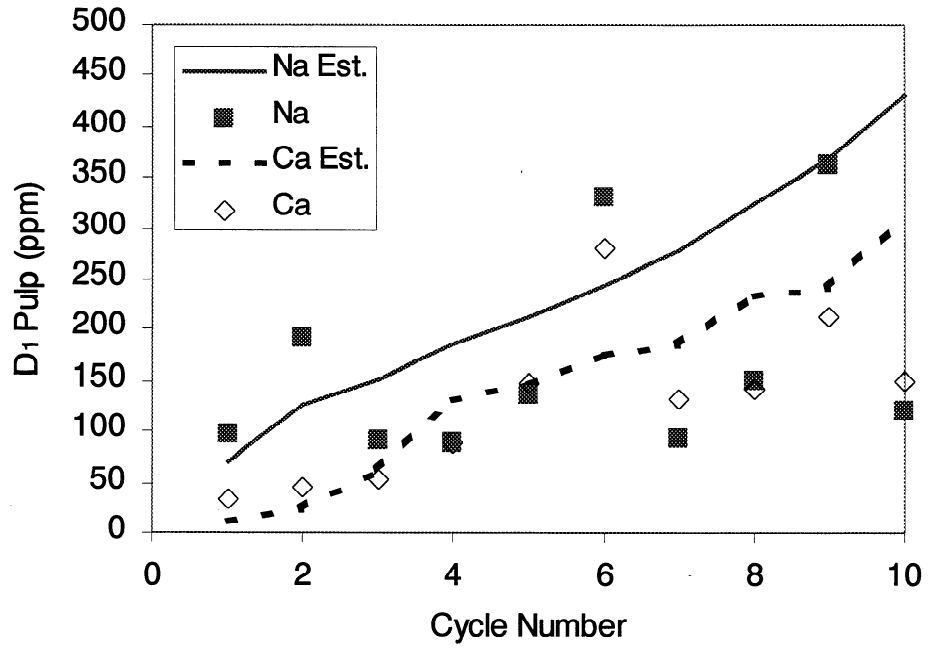


Fig. 10

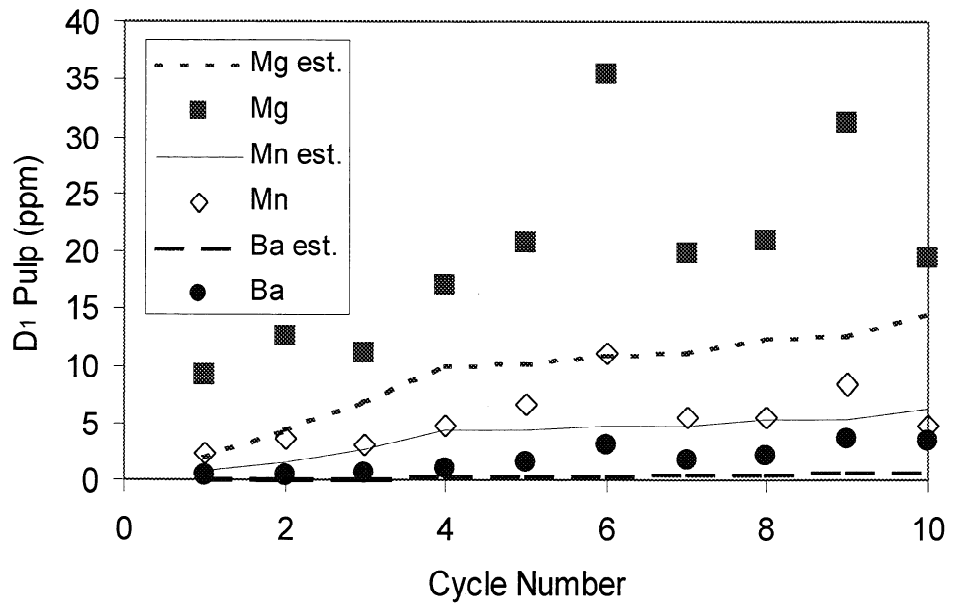


Fig. 11

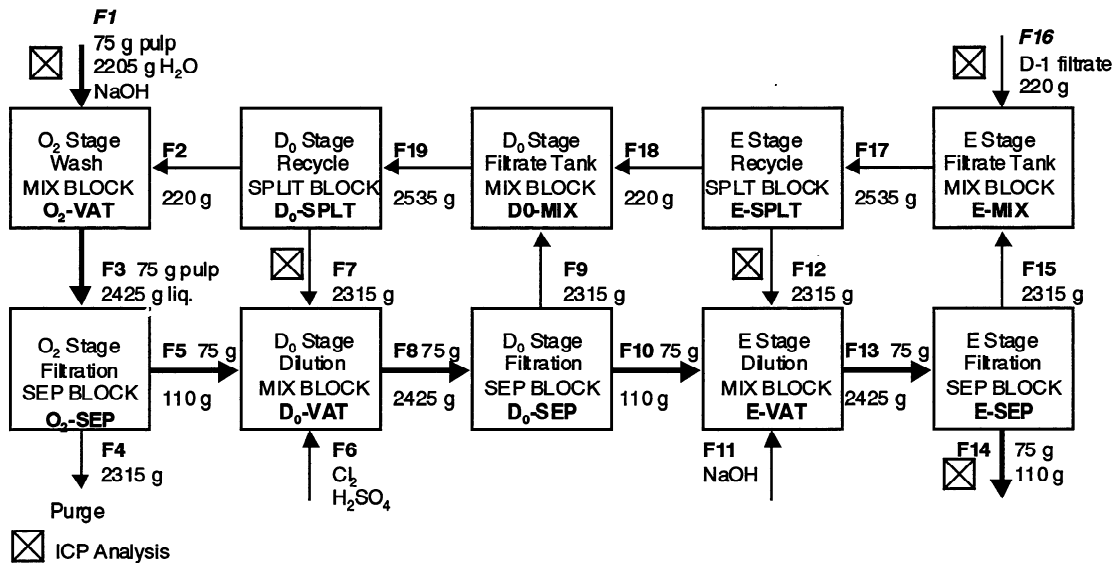


Fig. 12a

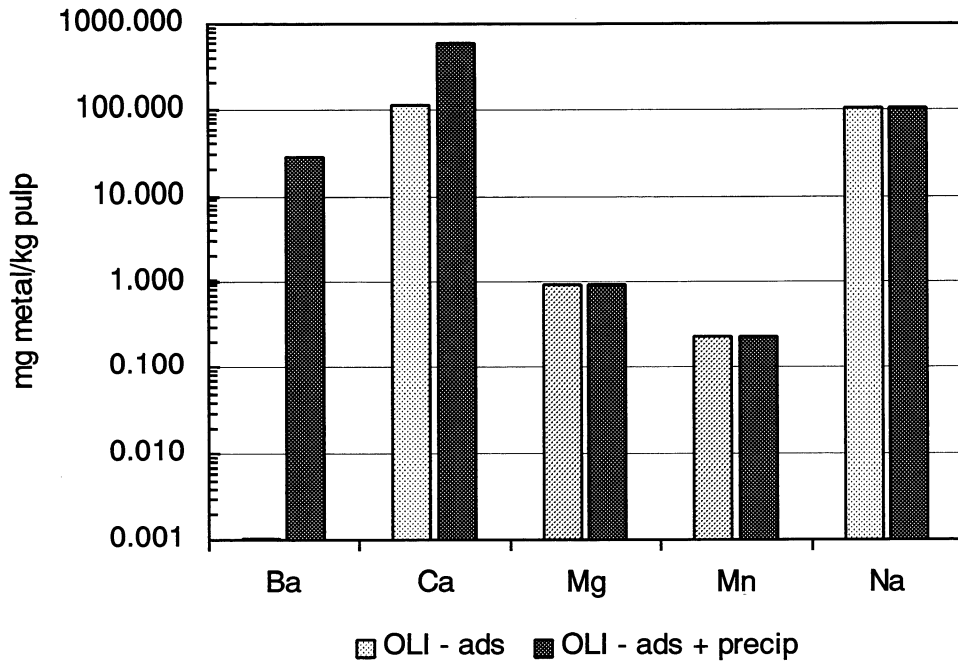


Fig. 12b

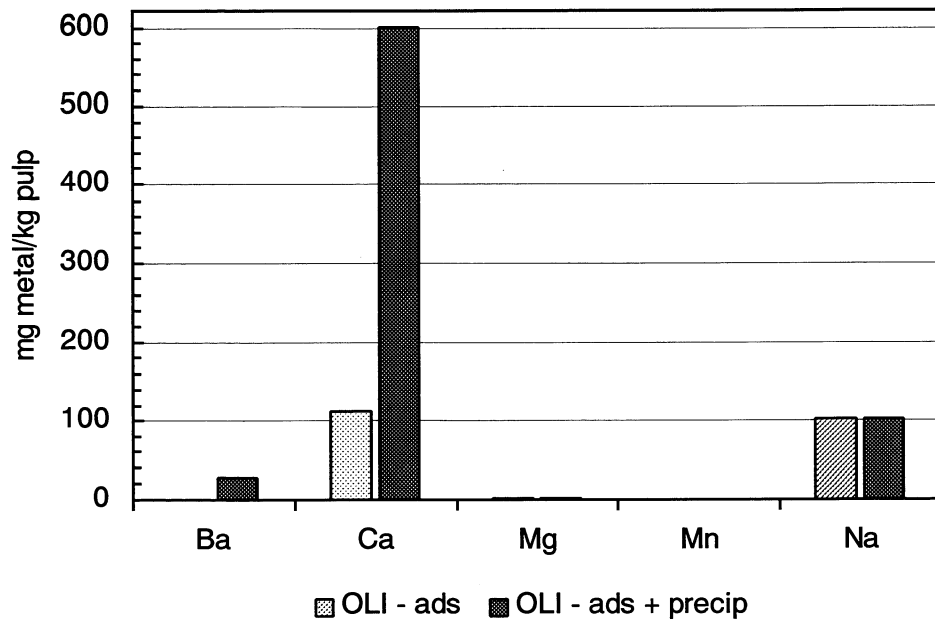


Fig. 13a

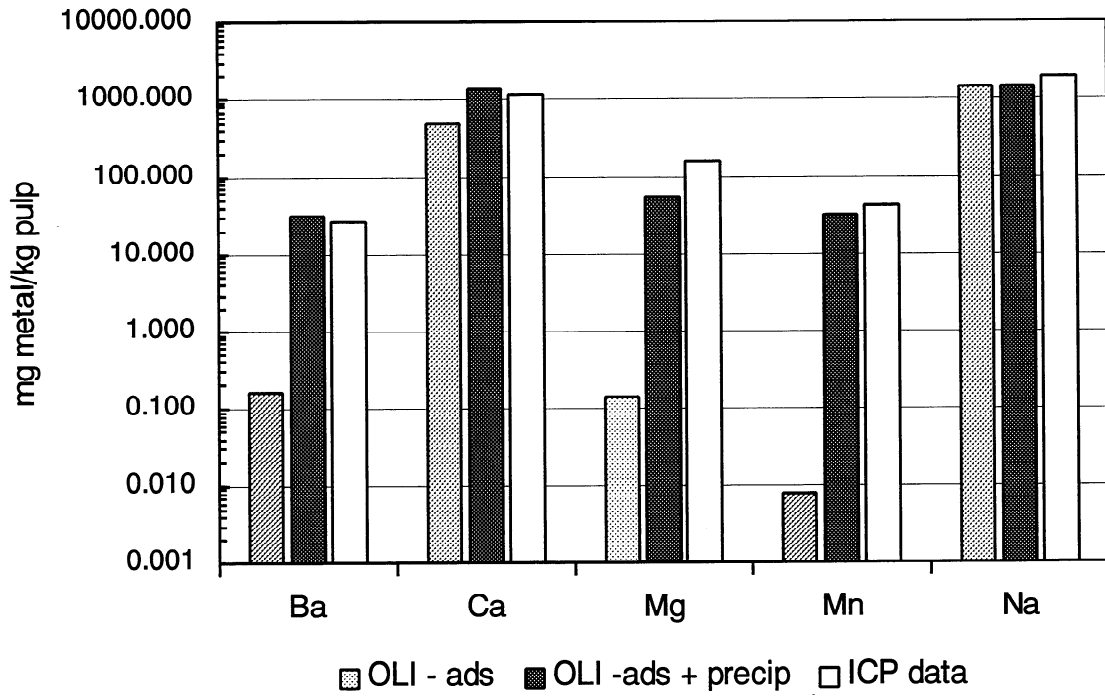


Fig. 13b

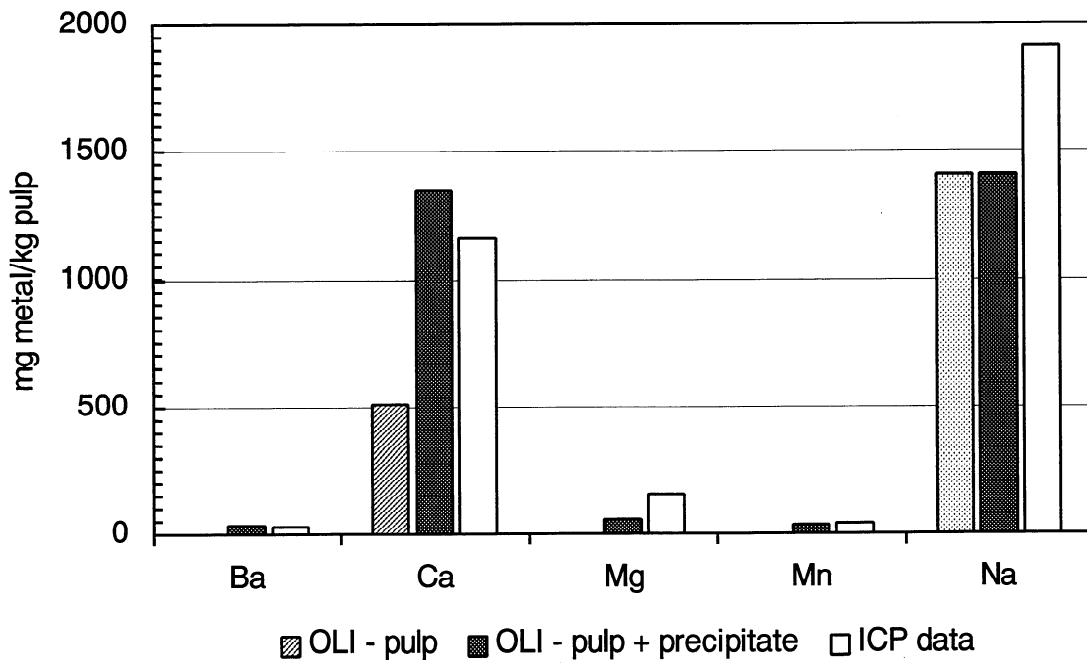


Fig 14a

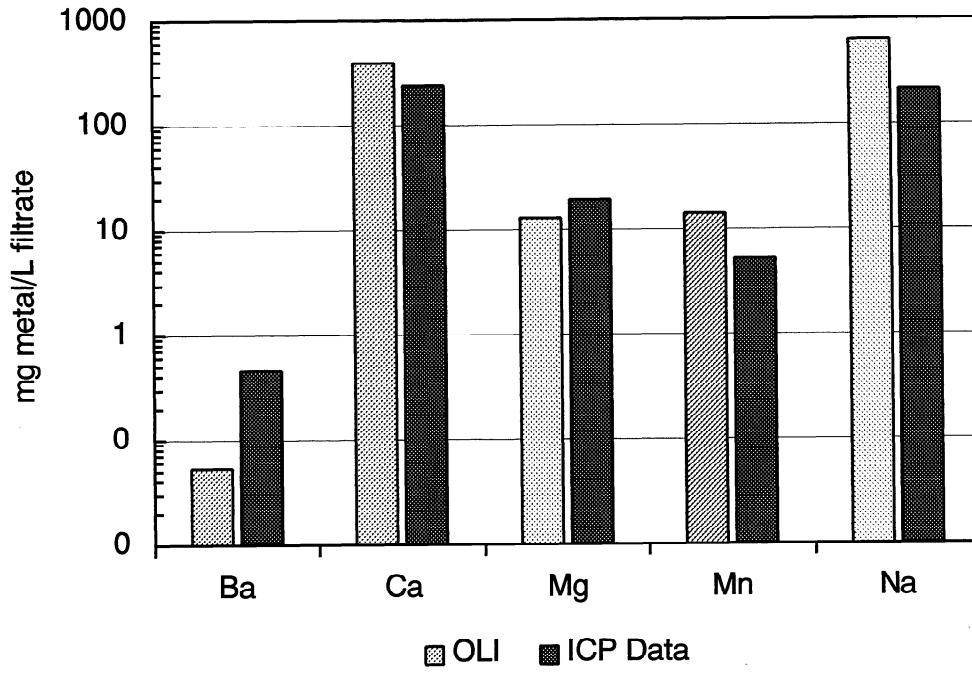


Fig. 14b

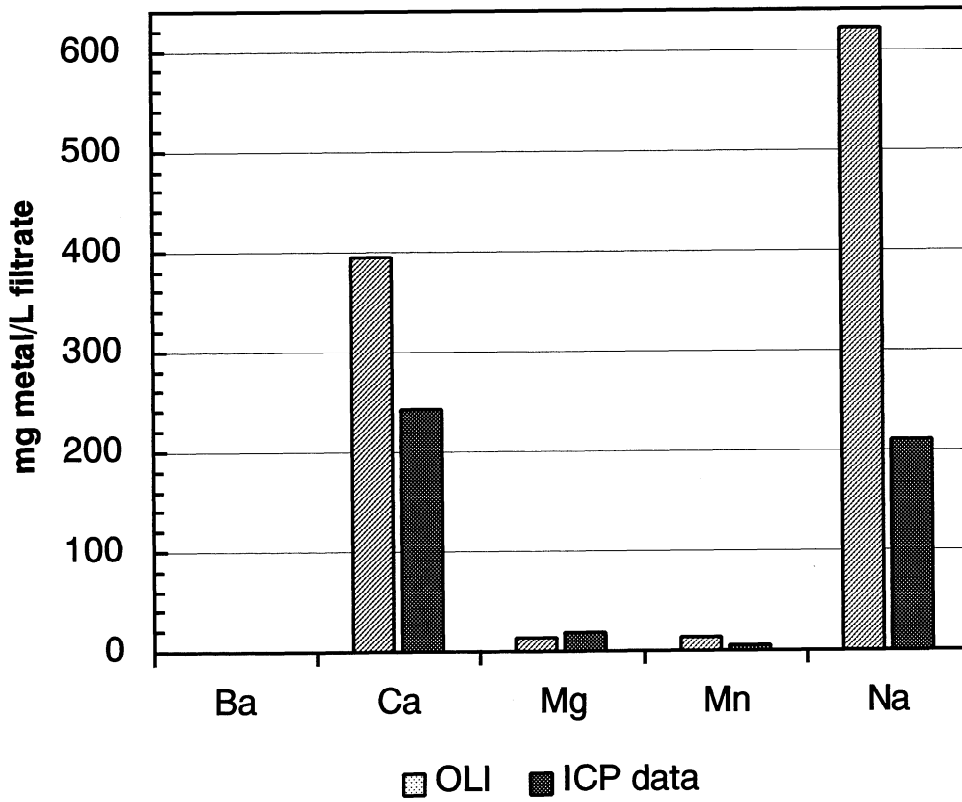


Fig. 15a

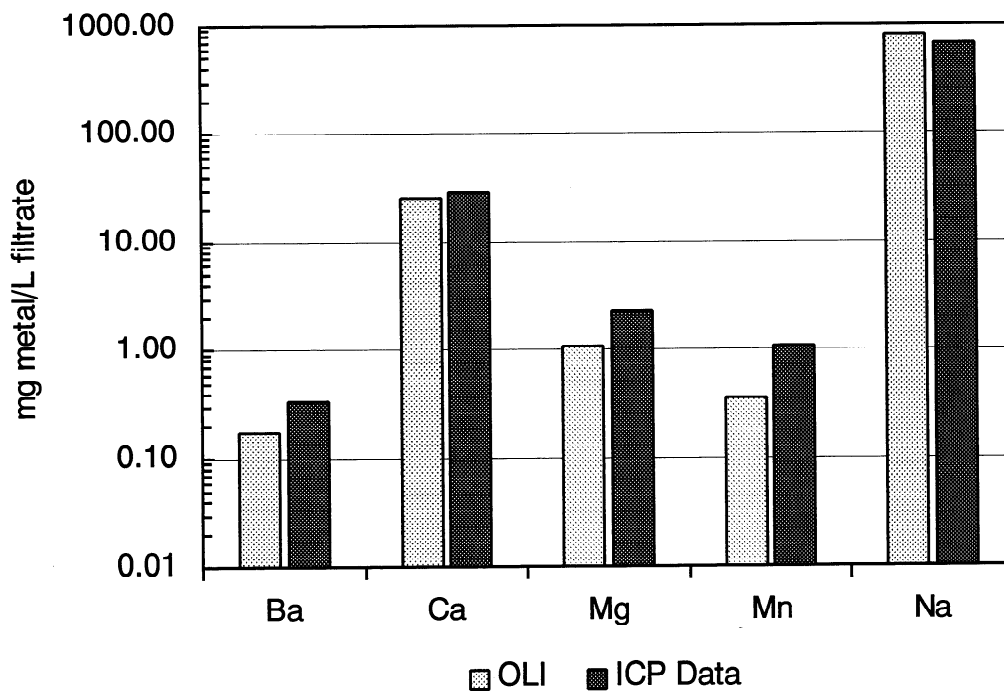


Fig. 15b

